Modeling Mn(II) autocatalytic sorption on MnOx-coated filtration media

Materials and methods: Supplemental information about the uptake column experiment.

Mini column description : diameter = 31.75 mm, media depth = 5.0 cm, volume = 119 cm3, EBCT = 0.13 min, VL= 23.5 m/h

Composition of the solution: 50 mg CaCO3/L of bicarbonate, 25 mg CaCO3/L of hardness

pH tested: 6.0, 6.5, 7.0, 7.5, 8.0, 8.5 and 9.0

Initial concentration tested: 0.50, 0.75, 1.00, 1.50 mg Mn/L

Temperature: 4 and 20°C

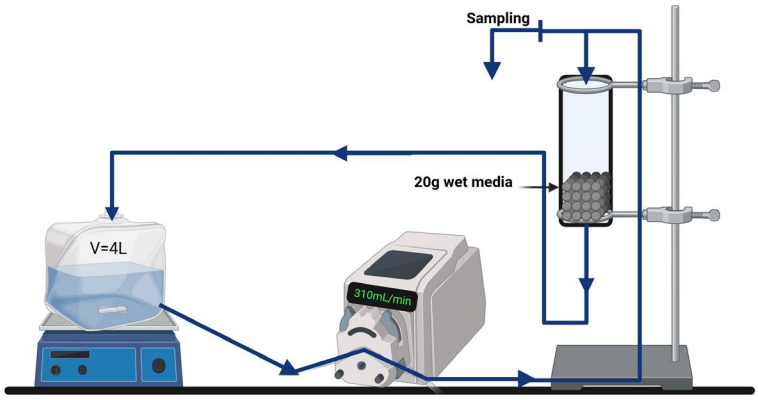

Figure S1. Experimental set-up for conducting the Mn(II) uptake experiments using small columns with downflow recirculation (created with Biorender.com).

Materials and methods: Supplemental information about the characterization of MnOx media

The media used in this study was collected from a pilot-scale manganese biofilter fed with groundwater (Saint-Donat, Canada) for six months in the spring of 2021. The influent Mn and Fe concentrations were 0.47±0.06 mg Mn/L and 0.2±0.1 mg Fe/L, respectively. The sampled media were stored at 4 °C in demineralized water for eight months. This storage method reduces the biological activity of the media by osmotic choc, while preventing possible changes to the MnOx coatings that can occur due to their exposure to disinfectants (such as NaOCl and NaOH) or autoclaving (Allard et al. 2017; McCormick et al. 2021; Yang et al. 2020).

To confirm the bacterial activity reduction after long-term storage, adenosine triphosphate (ATP) was measured in triplicate using a Quench-Gone Aqueous test kit (LuminUltra™). ATP was quantified in the supernatant of 3 × 5 g (wet weight) of a filtration media after sonication in phosphate buffer. The biological activity of the dry media was 12.0 ± 5.3 ng ATP/cm^3, which is negligible compared to the typical biological activity of surface water granular activated carbon biofilters (between 200 to 1000 ng ATP/cm^3) (Earle, Stoddart, and Gagnon 2023) or the Mn/Fe sand biofilter operating in the vicinity of Montreal (Canada) (380 ng ATP/cm^3).

The point of zero charge (pH_{pzc}) of the media was determined using a potentiometric titration method described previously (Cristiano et al. 2011; Tripathy, Kanungo, and Mishra 2001). The BET surface area and average pore size were calculated using N_2 adsorption isotherm analysis (TriStar II Plus™, micromeritics®). The media was characterized by X-Ray Diffraction (XRD) (D8 Advance, Bruker®), scanning electron microscopy coupled with energy dispersive X-ray spectroscopy (SEM-EDS) (FEG-SEM JSM-7600F™, Jeol®), and EDS X-max™ (Oxford Instruments®) at Polytechnique Montreal CM2 laboratories. These analyses were performed to

determine the mineralogy of the virgin media and to validate the presence of a MnOx coating around the media grains. The Mn content of the media was determined through atomic absorption spectroscopy using a PinAAcle 900F spectrometer (PerkinElmer). Prior to the analysis, samples were prepared by acid digestion using 15 mL of 12.4 M HCl added to 0.5 g of dry media and heated at 95°C for 2.5 h (Ducret and Barbeau 2024). Finally, electron paramagnetic resonance (EPR) spectra of the media before and after uptake were obtained using a homemade EPR spectrometer (Lacroix, 2010) operating at 9.4 GHz at room temperature (approximately 22°C). The spectrometer was designed, assembled, and operated at the Department of Physical Engineering at Polytechnique Montreal. The MnOx coating of the media was classified as biologically or chemically formed, according to the reference values proposed by Kim et al. (2011).

Results and discussion: Preliminary characterization of the aged media

The virgin media was a mixture of 92% quartz (SiO_2) and 8% albite ($NaAlSi_3O_8$) as identified by XRD (data not shown). After six months of operation in the pilot filter, the media was coated by a MnOx mesoporous layer (average pore diameter of 109 Å) of a depth of approximately 25 µm, as estimated by SEM-EDS (Figure S2). The nitrogen adsorption–desorption isotherms (Figure S1) exhibited a physisorption Type IV isotherm with H3 loops, according to the IUPAC classification (Thommes et al. 2015). Type-IV isotherms are characteristic of mesoporous adsorbents. The hysteresis loop is typical of "non-rigid aggregates of plate-like particles" (Thommes et al. 2015), corresponding to a wedge-shaped pore (Xu et al. 2020). The specific surface area determined by the BET desorption isotherm of N_2 at 77 K was 1.93 m^2/g. The point

of zero charge was calculated to be 2.6, while the Mn content and the relative density were respectively quantified as 5.7 ± 1.2 mg Mn/g and 2.649 ± 0.003.

The EPR spectrum from the media before the experiment exhibited a linewidth ΔH of 609 gauss, corresponding to the limit of the biotic origin, as defined by Kim et al. (2011). At the end of the uptake study, the five samples analyzed with EPR exhibited a mean linewidth ΔH of 1727 ± 479 gauss (> 1200 gauss), corresponding to an abiotic origin of the manganese oxides (Kim et al. 2011). This finding confirms that the Mn uptake during the column tests was due to abiotic mechanisms.

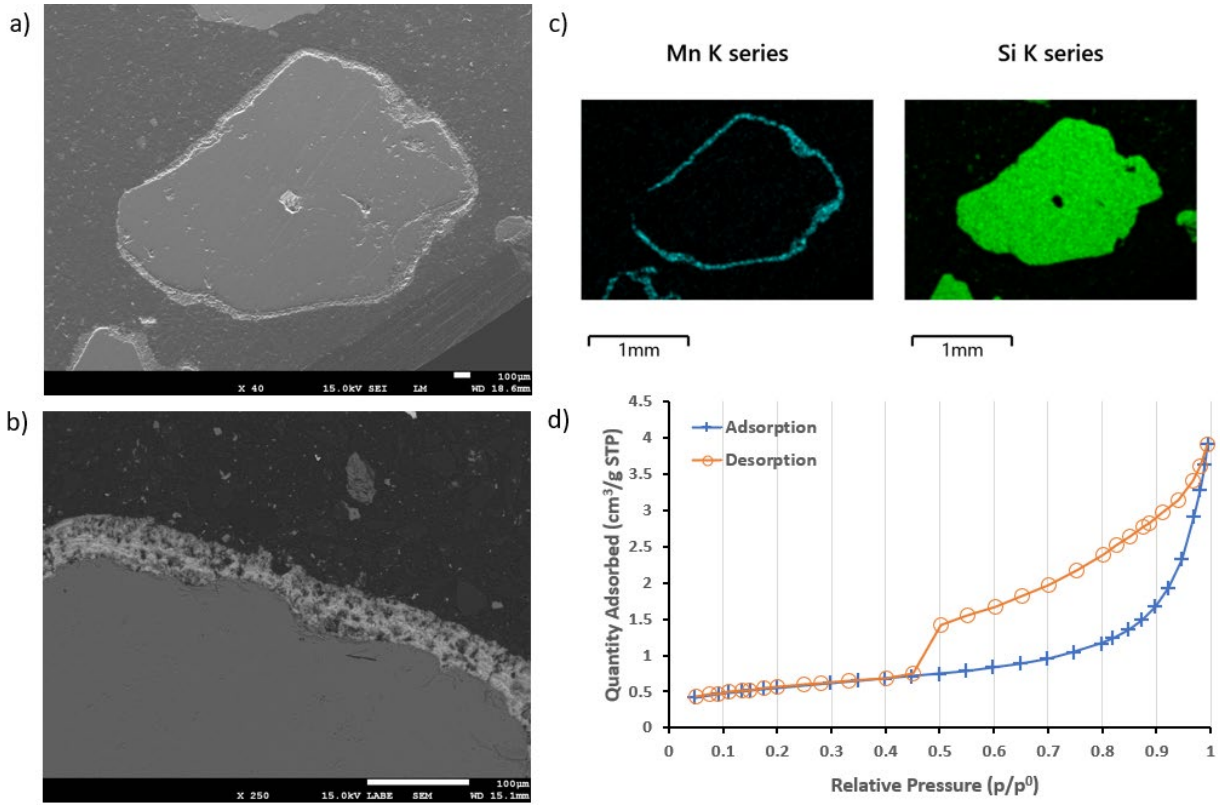

Figure S2. a) Scanning electron microscopy (x40) of the media studied, b) Scanning electron microscopy (x250) of the media studied, c) Mapping of Mn K series and Si K series of a grain of the media studied, d) Nitrogen adsorption and desorption isotherms (77K) for the media studied.

Table S1. Parameters of Freundlich and Langmuir isotherms for the abiotic uptake experiments for all conditions tested.

Temperature	**pH**	**Langmuir**			**Freundlich**		
		b (L/mg Mn)	q_{mL} (mg Mn/g)	R^2	K_f	n	R^2
4°C	6	3.0275	0.4290	0.9819	0.3382	1.784	0.9975
	6.5	7.2911	0.2757	0.7829	0.3000	2.444	0.9092
	7	2.2906	0.2432	0.9056	0.8412	2.1097	0.9429
	7.5	2.0805	0.2602	0.9328	0.1895	1.8886	0.8959
	8	3.1978	0.2027	0.9402	0.1574	2.6539	0.8879
	8.5	5.6609	0.3704	0.5811	0.3913	2.260	0.6431
	9	1.9790	0.5522	0.991	0.3999	1.697	0.9558
20°C	6	13.7278	0.3209	0.7995	0.4416	2.453	0.8782
	6.5	6.5191	0.4512	0.9935	0.5337	2.042	0.9978
	7	2.6361	0.3421	0.8152	0.2777	1.9171	0.799
	7.5	5.3731	0.2258	0.9192	0.2251	2.4295	0.9489
	8	2.4780	0.3329	0.9483	0.2523	2.0416	0.9244
	8.5	18.8686	0.3413	0.8723	0.4713	2.786	0.9297
	9	12.7044	0.3641	0.9509	0.4955	2.384	0.9867

Table S2. Pseudo first order kinetics and pseudo second order kinetics parameters for all the conditions tested.

		Pseudo first order kinetics				Pseudo second order kinetics			
Temperature (°C)	**C_0 (mg Mn/L)**	**k_1**	**R^2**	**Relative error on q_e (%)**	**Relative error on C(t) (%)**	**k_2**	**R^2**	**Relative error on q_e (%)**	**Relative error on C(t) (%)**
pH = 6									
4	0.5	0.0112	0.9949	9.3	16.7	0.4304	0.9727	22.0	20.0
	0.75	0.0119	0.9959	2.7	5.1	0.1738	0.9866	14.4	14.6
	1.0	0.0113	0.9948	4.1	6.2	0.1543	0.9840	17.2	12.6
	1.5	0.0116	0.9808	6.3	7.7	0.2592	0.9314	29.4	14.4
20	0.5	0.0155	0.9923	8.6	29.6	0.4021	0.9839	9.8	34.6
	0.75	0.0126	0.9936	11.8	22.1	0.2887	0.9785	14.9	17.9
	1.0	0.0126	0.9954	9.5	20.8	0.2005	0.9735	17.3	24.1
	1.5	0.0118	0.9930	5.3	8.8	0.1095	0.9885	15.3	14.5
pH = 6.5									
4	0.5	0.0118	0.9960	5.9	12.7	0.3349	0.9779	20.0	23.4
	0.75	0.0111	0.9951	0.2	2.7	0.0433	0.9999	39.7	1.9
	1.0	0.0108	0.9933	5.3	7.3	0.2567	0.9607	26.5	14.4
	1.5	0.0106	0.9874	6.3	6.7	0.2931	0.9172	32.6	12.4
20	0.5	0.0145	0.9964	7.8	23.3	0.2553	0.9889	6.8	26.6
	0.75	0.0137	0.9946	10.8	27.3	0.3053	0.9734	15.8	28.3
	1.0	0.0134	0.9924	8.1	16.9	0.2337	0.9662	19.6	25.1
	1.5	0.0125	0.9942	7.6	12.8	0.1204	0.9782	15.2	15.7
pH = 7									

4	0.5	0.0126	0.9863	13.6	22.7	0.2549	0.9974	0.2	7.5
	0.75	0.0103	0.9914	1.3	1.9	0.1045	0.9978	5.0	4.9
	1.0	0.0126	0.9852	0.3	2.0	0.7603	0.8222	37.7	9.6
	1.5	0.0097	0.9865	1.8	2.2	0.1687	0.9842	20.6	5.3
20	0.5	0.0123	0.9909	0.4	3.2	0.3142	0.9808	18.1	13.8
	0.75	0.0115	0.9887	9.5	12.7	0.0275	0.9827	86.5	16.7
	1.0	0.0112	0.9916	4.8	4.5	0.1004	0.9976	6.7	3.7
	1.5	0.0114	0.9886	1.6	2.8	0.1119	0.9878	14.7	7.5
pH = 7.5									
4	0.5	0.0143	0.9553	3.9	4.6	1.0180	0.9030	33.7	14.1
	0.5	0.0109	0.9858	12.5	7.0	-5.282	0.4951	86.3	25.5
	0.5	0.0099	0.9942	2.0	3.0	0.3229	0.9866	21.5	8.6
	0.75	0.0095	0.9951	2.5	3.2	0.4218	0.9028	35.5	10.8
	1.0	0.0105	0.9854	3.3	2.4	0.2361	0.9700	27.7	8.2
	1.5	0.0111	0.9901	4.4	5.5	0.1834	0.9675	26.0	12.4
20	0.5	0.0107	0.9943	2.2	3.5	0.4593	0.9606	27.9	12.4
	0.5	0.0122	0.9886	2.3	3.2	0.0008	0.9880	1085.0	61.6
	0.5	0.0111	0.9886	3.4	5.7	-1.856	0.8601	86.2	63.6
	0.75	0.0117	0.9971	4.1	4.6	0.2978	0.9778	20.0	10.0
	1.0	0.0111	0.9961	3.7	3.9	0.1915	0.9888	16.4	7.9
	1.5	0.0126	0.9938	5.3	8.7	0.1104	0.9762	15.3	15.0
pH = 8									
4	0.5	0.0120	0.9748	5.7	3.8	0.0691	0.9956	41.5	2.6
	0.75	0.0107	0.9940	3.1	3.2	0.3945	0.9522	28.1	9.3
	1.0	0.0091	0.9814	0.8	2.1	0.3653	0.9573	35.4	7.1

	1.5	0.0099	0.9867	13.1	4.9	-36.65	0.0050	93.1	16.5
20	0.5	0.0114	0.9969	1.9	3.5	0.1148	0.9992	12.7	4.7
	0.75	0.0114	0.9906	7.3	8.9	0.0674	0.9981	26.8	2.4
	1.0	0.0119	0.9865	5.1	3.5	0.0376	0.9794	195.8	304.0
	1.5	0.0096	0.9913	8.0	4.7	-2.582	0.1918	82.9	25.6
pH = 8.5									
4	0.5	0.0123	0.9940	1.8	2.9	0.6383	0.9606	26.5	11.6
	0.5	0.0129	0.9966	3.4	7.5	0.2410	0.9936	8.1	17.0
	0.75	0.0136	0.9832	8.5	21.9	0.3630	0.9552	21.5	35.3
	1.0	0.0111	0.9910	9.0	12.1	0.2768	0.9610	23.0	14.2
	1.5	0.0125	0.9923	2.7	5.4	0.2454	0.6554	38.9	26.5
20	0.5	0.0115	0.9800	2.6	6.7	1.8011	0.9185	108.7	123.0
	0.5	0.0141	0.9943	10.9	45.2	0.2348	0.9945	4.6	34.1
	0.75	0.0114	0.9974	4.2	4.9	0.2008	0.9828	12.1	8.4
	0.75	0.0136	0.9958	8.1	19.0	0.2107	0.9787	13.2	23.5
	1.0	0.0136	0.9949	11.8	28.2	0.2643	0.9445	20.1	30.3
	1.5	0.0117	0.9940	6.6	11.6	0.1474	0.9686	22.2	19.3
pH = 9									
4	0.5	0.0113	0.9969	5.9	10.8	0.3153	0.9836	16.4	16.8
	0.75	0.0123	0.9933	8.6	13.5	0.4488	0.9162	26.2	20.0
	1.0	0.0106	0.9983	4.8	8.5	0.1409	0.9853	16.5	14.9
	1.5	0.0114	0.9823	10.4	11.4	0.3334	0.9070	29.0	13.1
20	0.5	0.0160	0.9956	10.3	38.2	0.4025	0.9763	11.4	41.2
	0.75	0.0134	0.9915	13.1	30.6	0.2810	0.9747	14.5	23.7
	1.0	0.0134	0.9939	10.7	24.0	0.1985	0.9801	14.4	22.8

	1.5	0.0122	0.9937	9.2	15.1	0.1076	0.9925	10.6	12.9

Table S3. Adsorption-Oxidation kinetics parameters for all the conditions tested. For the generalized adsorption-oxidation model, bold values (n=15) were used for validation of the model while other values (n=48) were used for the calibration.

Temperature (°C)	**C_0 (mg Mn/L)**	**k_{ad}**	**k_{ox}**	**$q_{Mn2+,e}$**	**Relative error on C(t) (%)**
pH = 6					
4	0.5	0.04604	0.00545	0.06805	0.034
	0.75	0.02252	0.00353	0.12034	0.013
	1.0	0.02627	0.00440	0.13479	0.012
	1.5	0.06493	0.00742	0.13055	0.081
20	*0.5*	0.03414	0.00237	0.08529	0.074
	0.75	0.03848	0.00334	0.11415	0.038
	1.0	0.03478	0.00350	0.16333	0.061
	1.5	0.03413	0.00487	0.19259	0.059
pH = 6.5					
4	0.5	0.03025	0.00425	0.08254	0.027
	0.75	0.01754	0.00367	0.10624	0.002
	1.0	0.03250	0.00552	0.11049	0.020
	1.5	0.05455	0.00769	0.11614	0.043
20	0.5	0.02633	0.00187	0.11026	0.042
	0.75	0.04111	0.00339	0.12176	0.101
	1.0	0.04348	0.00434	0.15264	0.194
	1.5	0.03299	0.00366	0.22395	0.057
pH = 7					
4	*0.5*	0.03396	0.00251	0.08168	0.005

	0.75	0.01722	0.00521	0.07283	0.002
	1.0	0.02123	0.00380	0.08664	0.029
	1.5	0.04024	0.00978	0.06762	0.012
20	*0.5*	0.02062	0.00351	0.07506	0.012
	0.75	0.04194	0.00455	0.09472	0.024
	1.0	0.02295	0.00338	0.10427	0.012
	1.5	0.02258	0.00428	0.16166	0.023
pH = 7.5					
4	0.5	0.08591	0.01025	0.03139	0.070
	0.5	0.00435	0.00000	0.11055	0.014
	0.5	0.02641	0.00686	0.04925	0.004
	0.75	0.02434	0.00661	0.06295	0.005
	1.0	0.01304	0.00435	0.09766	0.006
	1.5	0.03703	0.00626	0.14461	0.041
20	0.5	0.02336	0.00510	0.05857	0.006
	0.5	0.01674	0.00306	0.08250	0.013
	0.5	0.00887	0.00077	0.12476	0.083
	0.75	0.02474	0.00383	0.08897	0.012
	1.0	0.02568	0.00460	0.10364	0.013
	1.5	0.02731	0.00334	0.22964	0.036
pH = 8					
4	0.5	0.01201	0.00297	0.07286	0.016
	0.75	0.02519	0.00507	0.07130	0.006
	1.0	0.03626	0.01129	0.04858	0.003
	1.5	0.00271	0.00000	0.30641	0.042
20	0.5	0.01958	0.00335	0.07612	0.001

	0.75	0.02743	0.00333	0.10302	0.011
	1.0	0.01170	0.00212	0.14668	0.006
	1.5	0.00528	0.00071	0.27813	0.089
pH = 8.5					
4	0.5	0.02156	0.00357	0.05885	0.021
	0.5	0.02361	0.00303	0.08453	0.028
	0.75	0.06859	0.00559	0.10145	0.286
	1.0	0.03695	0.00459	0.11499	0.033
	1.5	0.01912	0.00225	0.25142	0.102
20	0.5	0.02418	0.00403	0.06972	0.084
	0.5	0.03508	0.00257	0.11042	0.058
	0.75	0.02218	0.00330	0.09279	0.002
	0.75	0.03004	0.00267	0.14778	0.040
	1.0	0.04095	0.00328	0.18397	0.182
	1.5	0.03409	0.00464	0.20189	0.060
pH = 9					
4	0.5	0.02717	0.00398	0.07117	0.008
	0.75	0.03850	0.00429	0.09952	0.053
	1.0	0.02400	0.00424	0.13758	0.011
	1.5	0.07339	0.00653	0.12994	0.071
20	0.5	0.03571	0.00220	0.10324	0.105
	0.75	0.04433	0.00330	0.13210	0.076
	1.0	0.03867	0.00328	0.17195	0.098
	1.5	0.03895	0.00413	0.20734	0.058

Text S1:

Figure S3A present the variations of k_{ad} in function of pH, the dotted curve represents a second order model depending on pH value (Eq. S1) to predict the value of k_{ad} depending of pH (error on k_{ad} of 45.7% for the individual fit).

$$k_{ad} = B * pH^2 + D * pH + E \quad (S1)$$

Figure S3B present the variations of k_{ox} in function of temperature, the dotted curve represents the Arrhenius law applied to k_{ox} (Eq. S2) to predict the value of k_{ox} depending of temperature (error on k_{ox} of 39.3% for the individual fit).

$$k_{ox} = A * e^{-\frac{E_a}{RT}} \quad (S2)$$

Figure S3C present the variations of $q_{Mn(II),e}$ in function of C_0 and temperature, the dotted curve represents an empirical model second order model (Eq. S3) depending on the temperature and the initial concentration (error on k_{ad} of 24.4% for the individual fit).

$$q_{Mn(II),e} = F * C_0^{\,G*(T-H)} \quad (S3)$$

The generalizable version of the adsorption-oxidation model is described by combining the Equation 3.12 with the Equation S1, S2 and S3. The letter A to H are the constants of the generalizable adsorption-oxidation model.

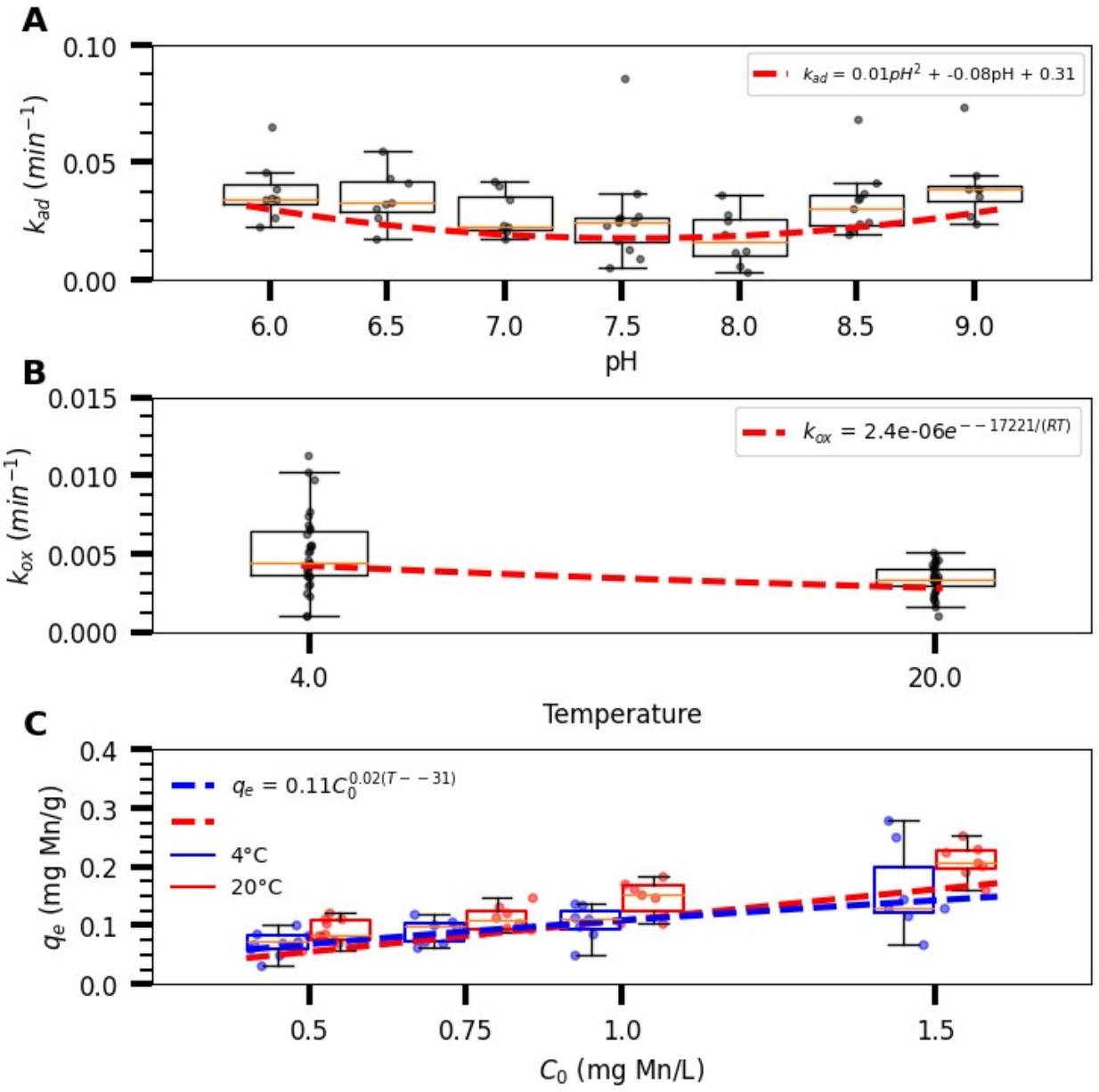

Figure S3. Variations of the constant determined by individual fit for each uptake column (n=64) for the operational conditions statistically impacting the parameters, the dotted curves represent the model used for the constant (Eq S1, Eq S2 and Eq S3). A) k_{ad} in function of pH. B) k_{ox} in function of temperature. C) $q_{Mn(II),e}$ in function of initial concentration and temperature.

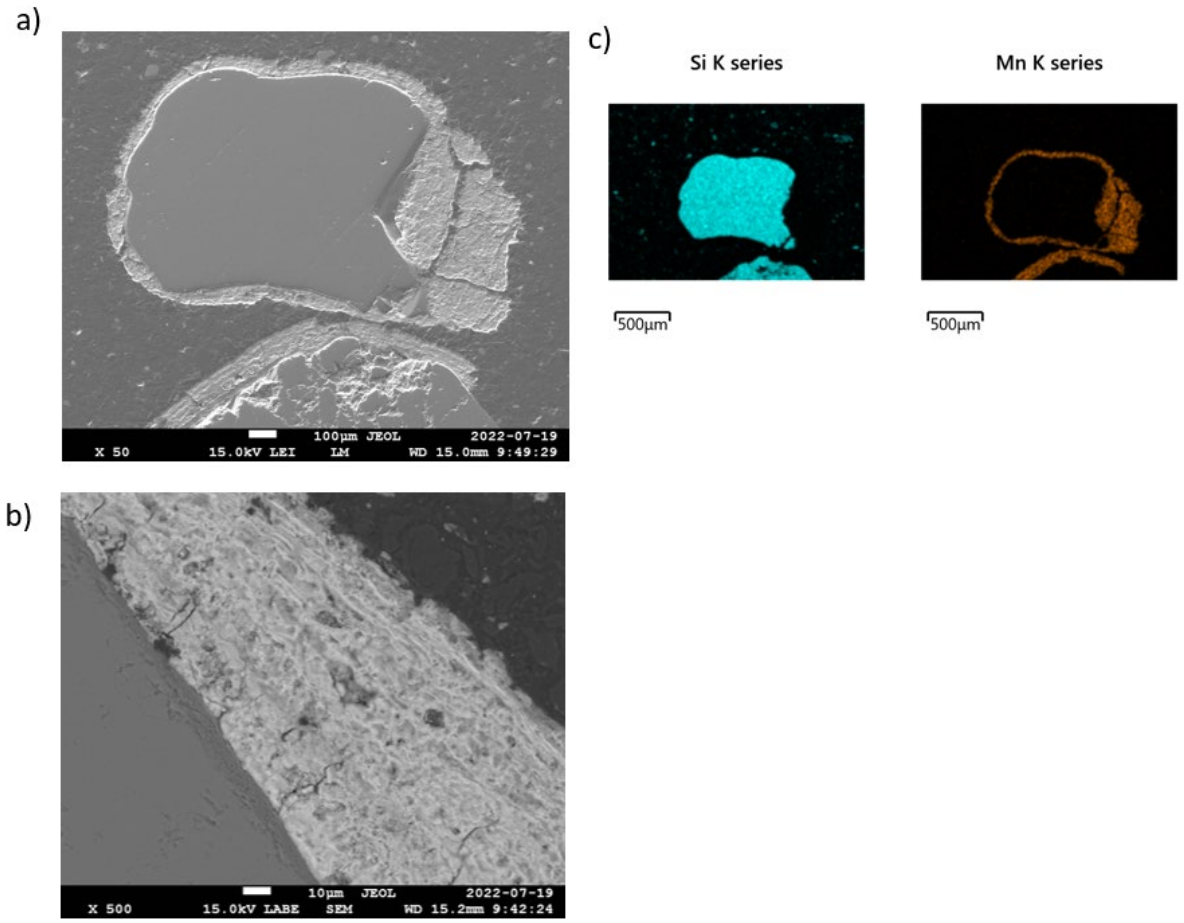

Figure S4. a) Scanning electron microscopy (x50) of the 6-years old media studied, b) Scanning electron microscopy (x500) of the 6-years old media studied, c) Mapping of Mn K series and Si K series of a grain of the media studied. PZC = 5.1 (potentiometric titration), Manganese content = 32±3 mg Mn/g (acid digestion) and EPR signal from the media before the experiment linewidth ΔH = 2406 gauss, corresponding to a physico-chemical origin (Kim et al., 2011).

Table S4. Adsorption-Oxidation kinetics parameters for all the conditions tested on the 6-years old media.

Temperature (°C)	**C_0 (mg Mn/L)**	**k_{ad}**	**k_{ox}**	**$q_{Mn2+,e}$**	**Relative error on C(t) (%)**
pH = 7					
4	0.5	0.0008	0.0001	0.6665	0.13
20	0.5	0.0024	0.0001	0.5491	0.07
pH = 7.5					
4	0.5	0.0069	0.0101	0.1738	0.02
	0.75	0.9221	0.0216	0.0811	0.24
	1.0	0.0019	0.0019	0.6773	0.01
	1.5	0.0144	0.0075	0.3423	0.39
20	0.5	0.0027	0.0001	0.5939	0.05
	0.75	0.0019	0.0001	0.8301	0.07
	1.0	0.0029	0.0007	0.9421	0.16
	1.5	0.0023	0.0013	1.3029	0.03
pH = 8					
4	0.5	0.0026	0.0057	0.2954	0.01
20	0.5	0.0026	0.0003	0.5177	0.03

Text S2:

Statistical analyses (Kruskal-Wallis) were performed to determine the impact of the different conditions on the three parameters of the model. No operational conditions tested in this article impact statistically the k_{ad} value, so we chose a value of k_{ad} constant. While temperature impact statistically k_{ox} (p-value = 0.028), so we used an Arrhenius law (Eq. S2) to traduce the effect of temperature on k_{ox}.

The effect of temperature on $q_{Mn(II),e}$ is not statistical at 95%, but close (p-value = 0.055). While the initial concentration impact did not impact statistically the value of $q_{Mn(II),e}$ (p-value = 0.31). We chose to use the same equation (Eq. S3) as for the 6-months media for $q_{Mn(II),e}$ because it's remains a system submitted to the isotherm equilibrium.

The three equations used in this model give the best results in simulations (other equations have been tested).

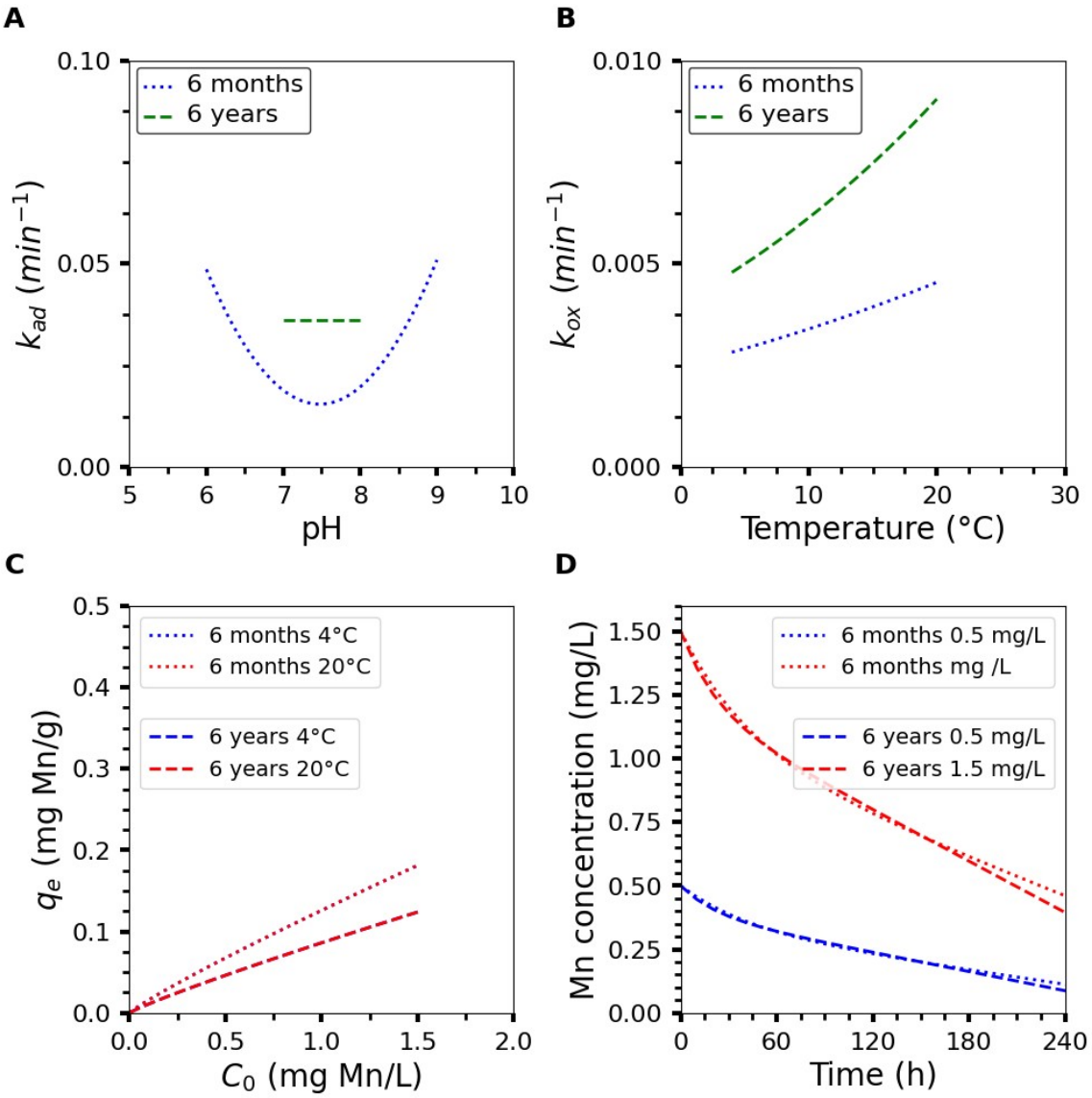

Figure S5. Variations of the fitted parameters as a function of significant operational parameters for both studied media: A) Variations of k_{ad} as a function of pH, B) k_{ox} as a function of temperature, C) and q_e as a function of initial concentration and temperature (results for both temperatures are superimposed). D) Simulated Mn(II) concentration using the adsorption–oxidation model for uptake at 20 °C at pH 7 for initial Mn(II) concentrations of 0.5 and 1.5 mg/L for both media.

REFERENCES

Allard, S., L. Gutierrez, C. Fontaine, J. P. Croue, and H. Gallard. 2017. 'Organic matter interactions with natural manganese oxide and synthetic birnessite', Sci Total Environ, 583: 487-95.

Cristiano, Elena, Yung-Jin Hu, Matthew Sigfried, Daniel Kaplan, and Heino Nitsche. 2011. 'A Comparison of Point of Zero Charge Measurement Methodology', Clays and Clay Minerals, 59: 107-15.

Ducret, Jérôme, and Benoit Barbeau. 2024. 'A revised digestion method to characterize manganese content in solids', MethodsX, 12: 102731.

Earle, Martin, Amina Stoddart, and Graham Gagnon. 2023. 'Raw water biofiltration for surface water manganese control', Scientific Reports, 13.

Kim, S. S., J. R. Bargar, K. H. Nealson, B. E. Flood, J. L. Kirschvink, T. D. Raub, B. M. Tebo, and M. Villalobos. 2011. 'Searching for biosignatures using electron paramagnetic resonance (EPR) analysis of manganese oxides', Astrobiology, 11: 775-86.

Lacroix, Christian. 2010. 'Propriétés Magnétiques de Nanoagrégats Ferromagnétiques Encastrés dans une Épicouche Semi-Conductrice', Polytechnique Montréal.

McCormick, N. E., M. Earle, C. Ha, L. Hakes, A. Evans, L. Anderson, A. K. Stoddart, M. G. I. Langille, and G. A. Gagnon. 2021. 'Biological and physico-chemical mechanisms accelerating the acclimation of Mn-removing biofilters', Water Research, 207: 117793.

Thommes, Matthias, Katsumi Kaneko, Alexander V. Neimark, James P. Olivier, Francisco Rodriguez-Reinoso, Jean Rouquerol, and Kenneth S. W. Sing. 2015. 'Physisorption of gases, with special reference to the evaluation of surface area and pore size distribution (IUPAC Technical Report)', 87: 1051-69.

Tripathy, Sushree Swarupa, Sukriti Bhusan Kanungo, and Santosh Kumar Mishra. 2001. 'The electrical double layer at hydrous manganese dioxide/electrolyte interface', Journal of Colloid and Interface Science, 241: 112-19.

Xu, Longfei, Yiyi Zhang, James Ding, Liu, Yong Shi, Zhenwang Li, Yudong Dang, Nai-Chen Cheng, and Baosu Guo. 2020. 'Pore Structure and Fractal Characteristics of Different Shale Lithofacies in the Dalong Formation in the Western Area of the Lower Yangtze Platform', Minerals, 10: 72.

Yang, Haiyang, Zhongsen Yan, Xing Du, Langming Bai, Huarong Yu, An Ding, Guibai Li, Heng Liang, and Tejraj M. Aminabhavi. 2020. 'Removal of manganese from groundwater in the ripened sand filtration: Biological oxidation versus chemical auto-catalytic oxidation', Chemical Engineering Journal, 382: 123033.